Article

Effects of Hybrid Rockwool–Wood Fiber on the Performance of Asbestos-Free Brake Friction Composites

Nan Wang [1,2] ![ORCID], **Hao Liu** [2,3,*] **and Fei Huang** [2]

1   School of Mechanical and Electrical Engineering, China University of Mining and Technology, Xuzhou 221000, China
2   School of Mechanical and Electronic Engineering, Suzhou University, Suzhou 234000, China
3   Technology and Research Center of Engineering Tribology, Suzhou University, Suzhou 234000, China
*   Correspondence: lb20050011@cumt.edu.cn; Tel.: +86-18305573654

Abstract: The present study explores the physical-mechanical and tribological properties of hybrid wood fiber and rockwool-reinforced asbestos-free resin-based friction materials. We developed asbestos-free brake friction composites with different contents of hybrid fiber (wood and rockwool fiber) at a total fixed fiber loading of 30%. Then, the developed composites were investigated on the physical, mechanical, and tribological properties according to the industry standards. The results show that, with the increase in wood fiber, the density, hardness, and strength decrease, and the water absorption increases. Meanwhile, rockwool fiber can improve the coefficient of friction and enhance friction stability, while wood fiber has a significant impact on wear resistance. The sample with 5% wood fiber and 25% rockwool fiber presented the best performance in terms of the coefficients of friction, wear rate, and fade–recovery behavior. It provides a new idea for the research of asbestos-free composites.

Keywords: hybrid fiber; asbestos-free; brake; friction composites

1. Introduction

Brake friction material is a kind of polymer composite, which is mainly composed of adhesive, reinforcement, friction modifier, and filler; the tribology performance directly affects the reliability and stability of the brake system [1,2]. Among many components, reinforcing fibers play an important role in the physical and mechanical properties of composites; meanwhile, they can improve thermal stability, lubrication, and wear resistance [3,4]. Although asbestos fiber has excellent braking performance, it has been banned owing to its harmful effects on the human respiration system [5,6]. Therefore, asbestos fiber substitutes have become the focus of friction composites.

In recent years, natural and synthetic fibers such as plant fiber [7,8], animal fiber [9], mineral fiber [10], glass fiber [11,12], carbon fiber [13], metal fiber [14,15], etc., have been added into composites to explore their effects on tribological properties. Among them, wood fiber has been widely used in the field of composite materials for the advantages of being a common source, its simple preparation, and its low price. Ibrahim [16] studied the influence of wood flour content on the tribological properties of polypropylene composites and found that, with the increase in wood flour content, the interface bonding ability of the composites was improved, and their wear resistance and mechanical properties were enhanced. Mazzanti [17] investigated the effect of the toughening agent on the wear resistance of a WPC and found that the brittleness declined with the addition of a toughening agent, causing the increase in wear resistance. By adding wood fiber to the ultra-high-molecular-weight polyethylene composite, Du [18] found that the friction coefficient and wear rate of the composite decreased significantly, and the modified wood fiber showed better performance. Amirthan [19] prepared five kinds of ceramic composites

based on natural fibers and found that coarse teak particles can cause the composites to show a very low wear rate and friction coefficient under dry sliding conditions.

Rockwool fiber is an important kind of mineral fiber with excellent chemical resistance, vibration resistance, noise resistance, thermostability, and high tensile strength that has been wildly used in brake friction materials [20,21]. Liu [20] studied the effects of different rockwool contents on the properties of friction composites and found that rockwool can significantly increase the friction coefficient and inhibit heat fading; meanwhile, the 9% fiber content has the lowest wear rate and best wear resistance. Stephen [21] investigated the influence of rockwool hybrid steel fiber on the performance of brake pads. The results show that the combination of 12% steel fiber and 8% rockwool fiber has the best tribological performance. Through the research on the morphology and distribution of rockwool, Makni [22] found that a regular size and distribution of rockwool balls induce better tribological behavior and enhance wear resistance. Aranganathan [23] prepared copper-free and copper-based brake pads reinforced with different contents of rockwool and concluded that the inclusion of rockwool and thermographite can replace Cu in friction materials; meanwhile, it can match the performance to a significant level.

However, due to the inherent characteristics of a single fiber, it is difficult to find a substitute fiber that can simultaneously meet the requirements of having excellent physical, mechanical properties, and tribological properties, as well as being low-cost and protecting the environment; therefore, fiber intermixing is the focus of future research [3,24]. It can be seen from the previous research that wood fiber can form carbon film during friction, effectively improving the wear resistance of composite materials, and making up for the defect of the high wear rate of rockwool. Therefore, in this work, wood fiber and rockwool fiber were mixed with different contents to prepare the brake friction composites; meanwhile, we studied the impact of hybrid fibers on the physical, mechanical, and tribological properties of the asbestos-free brake friction composites. Further, the study of the microstructure after friction was carried out with scanning electron microscopy (SEM) to explore the wear mechanism. This study provides a reference for environment-friendly, low-cost, and efficient fibers to enhance the performance of brake pads through hybrid materials.

2. Experimental Details

2.1. Materials and Composite Preparation

The wood fiber and rockwool were purchased from Jinli Mining Co., Ltd (Shijiazhuang, China) and Boyuan Ceramic Fiber Co., Ltd. (Jiaozuo, China), respectively. Their microstructures are presented in Figure 1. The developed friction material formula contains six constant components and two variable components; the specific components and functions are shown in Table 1. The process to prepare the brake pads was as follows: Firstly, the raw materials were weighed and mixed in the plough harrow mixer for 15 min; Secondly, they were hot pressed under 14.4 MPa at a temperature of 155 °C with four exhausts and maintained for another 4 min; Finally, they were heated in an oven at 130 °C for 2 h in the first phase, 160 °C for 3 h in the second phase, then cooled to room temperature in the third phase. The three friction samples were numbered W05R25, W10R20, and W15R15 according to the fiber content, respectively.
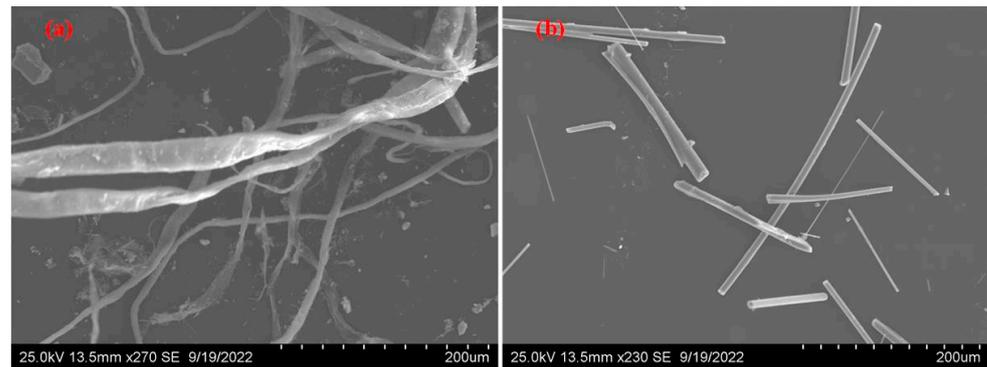
Figure 1. The microstructures: (**a**) wood fiber; (**b**) rockwool.

Table 1. Formulations of developed friction composites.

Ingredients (%)	Functions	Samples		
		W05R25	**W10R20**	**W15R15**
Phenolic resin	Binder	10	10	10
Rubber		3	3	3
Wood fiber	Reinforced fiber	5	10	15
Rockwool		25	20	15
Alumina	Abrasive	5	5	5
Graphite	Lubricant	6	6	6
Vermiculite	Filler	5	5	5
Barite		41	41	41

Note: the mass measurement accuracy is 0.01 g.

2.2. Characterization of Physical and Mechanical Properties

The physical and mechanical properties of the developed samples, including density, water absorption, hardness, and shear strength, were tested according to industry standards.

The density was measured according to the Archimedes drainage method, with a density balance (GP-300S, Xiongfa Instrument Co., Ltd., Xiamen, China), according to the JC/T 685-2009 standard. The samples were cut and polished to a size of 25 mm * 25 mm * 7 mm, with a smooth surface, and then placed in an indoor environment with a temperature of $25 \pm 5\,^\circ$C and relative humidity of 45–70% for density testing.

The water absorption was measured according to the ASTM D 570-98 standard, and the samples were immersed in a container of distilled water maintained at a temperature of $23 \pm 1\,^\circ$C for 24 h to test the mass change with a balance with an accuracy of 0.001 g.

The hardness was measured by the Rockwell hardness tester (HR-150A, Wenzhou Weidu Electronics Co., Ltd., Wenzhou, China) according to the GB/T 5766-2007 standard. In the indoor environment of $23 \pm 2\,^\circ$C and $50\% \pm 5\%$ relative humidity, five uniform distributed surface points without defects were selected for measurement, and then the average hardness value was taken.

The shear strength was measured using the shear strength tester (XJ-A, Xianyang Xinyi friction & sealing Equipment Co., Ltd., Xianyang, China) according to the GB/T22309-2008 standard. Firstly, the back of the sample was kept flat, and then the test was conducted under an ambient temperature of $23 \pm 5\,^\circ$C, a loading rate of 4500 ± 1000 N/s, and an indenter moving rate of 10 ± 1 mm/min. The measurements were repeated three times for the same sample to take the average value.

2.3. Friction and Wear Testing

In this work, the samples were cut into a size of 25.4 mm $\times$ 25.4 mm $\times$ 6 mm (as shown in Figure 2) for an assessment of the tribological properties, according to the GB/T

17469-2012 standard, with the Chase machine (XJ-A, Xianyang Xinyi friction & sealing Equipment Co., Ltd, Xianyang, China) [4–6]. The test procedure consisted of eight stages: Burnish, Baseline, Fade-I, Recovery-I, Wear, Fade-II, Recovery-II, and Baseline, in sequence. The detailed test parameters of the GB/T 17469-2012 standard are shown in Table 2. In the Fade-I cycle, the temperature increased from 93 °C to 288 °C, with an increase of 28 °C by the heater; similarly, in the Fade-II cycle, the temperature increased from 93 °C to 343 °C, with an increase of 28 °C by the heater. In the Recovery-I cycle, the temperature decreased from 260 °C to 93 °C, with a decrease of 56 °C by the fan; in the Recovery-II cycle, the temperature decreased from 316 °C to 93 °C, with a decrease of 56 °C by the blower.
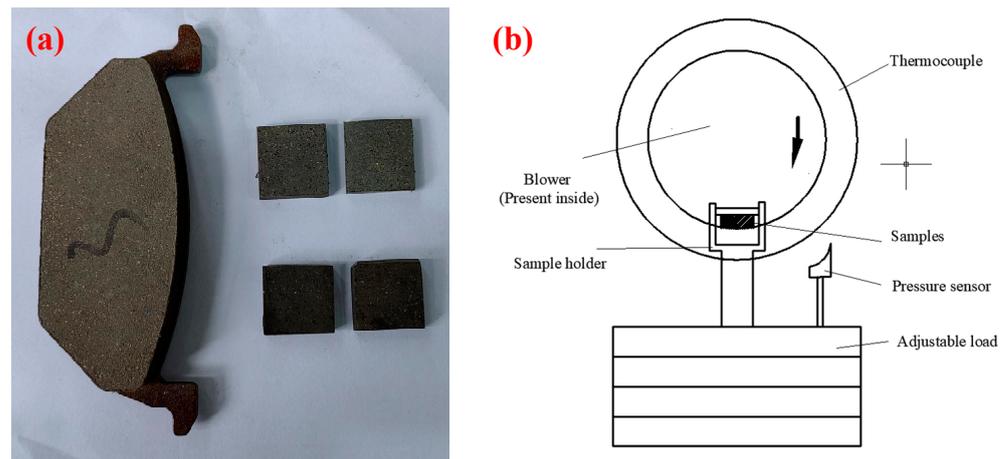

Figure 2. (**a**) A test sample of a brake pad and (**b**) the structure diagram of the test machine.

Table 2. The specific process and parameters of the Chase test.

Cycle	Speed (rpm)	Load (N)	Time		Temperature (°C)			Applications	Heater
			On	Off	Min	Max	Change		
Burnish	312	440	20 min	-	-	93		1	
Baseline	417	667	10 s	-	82	104		20	
Fade-I	417	667	10 min	-	93	288	28	1	on
Recovery-I	417	667	10 s	-	260	93	56	1	
Wear	417	667	20 s	10 s	193	204		100	
Fade-II	417	667	10 min	-	93	343	28	1	on
Recovery-II	417	667	10 s	-	316	93	56	1	
Baseline	417	667	10 s	20 s	82	104		20	

Note: the accuracy of the speed, load, and temperature measurement system is ±2% of the full scale.

The mass loss rate and thickness loss rate were calculated to evaluate the wear properties. The mass loss rate is defined as the ratio of mass loss and original mass. Meanwhile, the thickness loss rate is defined as the ratio of thickness loss and original mass. Samples with a lower wear rate have a longer service life.

3. Results and Discussion

3.1. Physical and Mechanical Characterization

Table 3 shows the physical and mechanical properties of the three developed samples. It can be seen that, with the increase in wood fiber content, the density of the samples gradually decreases. The W05R25 sample has the largest density (2.31 g/cm^3), while the W15R15 sample has the smallest (2.19 g/cm^3), due to the lower density of wood fiber than mineral fibers and the voids caused by intertwining natural fibers [25–27]. However, the wood fiber content does not exceed 15wt.% of the total amount, so it has a small impact on the overall density of the friction composites. Meanwhile, water absorption has the opposite trend, the W05R25 sample has the lowest level (0.58%), and the W15R15 sample

has the highest level (1.98%). The water absorption changes with the wood fiber content, mainly due to the hydrophilicity of plant fibers and its greater number of pores [7,28]. The hardness of the samples decreases with the increase in wood fiber: the W5R25 sample has the highest value (88.3), and W15R15 has the lowest value (77.3). This is mainly because rockwool is harder than wood fiber, and hard material has a positive relationship with the hardness of the composites and the good dispersion of rockwool [1,27,29]. The shear strength of the samples remains at a high level but decreases with the increase in wood fiber content (7.36–6.8). This is mainly due to the strength of the wood fiber being lower than that of rockwool and the poor combination of the intertwining fibers [30].

Table 3. The physical and mechanical properties of the developed samples.

Samples	Density (g/cm^3)	Water Absorption (%)	Hardness (HRR)	Shear Strength (MPa)
W05R25	2.31	0.58%	88.3	7.36
W10R20	2.27	1.02%	83.2	7.21
W15R15	2.19	1.98%	77.3	6.80

3.2. Friction and Wear Properties during Fade–Recovery Cycles

3.2.1. Friction Performance of the Composites

The friction coefficient curve during the fade–recovery cycles is shown in Figure 3. It can be observed that in the Fade-I cycle, with the increase in temperature, the friction coefficient has a gradual downward trend for the three samples. However, there are some differences. For the W05R25 sample, the friction coefficient keeps steady at 177 °C, slowly drops to 260 °C, and then remains stable (0.4). For the W10R20 sample, the friction coefficient gradually drops to 177 °C, with a slight rise to 204 °C, and then rapidly descends to the end. The W15R15 sample slowly descends to 204 °C, then rapidly descends to the end. In the Fade-II cycle, the friction coefficient for the W05R25 sample remains stable until 232 °C and then declines from 0.462 to 0.418. The friction coefficient for the W10R25 and W15R15 samples follows a similar trend, first rising to 204 °C, then declining to the end, except the W15R15 sample has a larger decline.

In the Recovery-I cycle, the friction coefficient for the W05R25 sample is basically stable with a small increase from 260 °C to 204 °C and a slow decrease to the end. The friction coefficient for the W10R25 and W15R15 samples rapidly rises from 260 °C to 149 °C and then remains stable. In the Recovery-II cycle, the friction coefficient for the W05R25 and W15R15 samples increases from 343 °C to 316 °C and then decreases to the end. The friction coefficient for the W10R20 sample decreases from 343 °C to 316 °C and remains basically stable between 260 °C and 149 °C, then decreasing to the end.

The friction coefficient value for the three samples during the fade–recovery cycles was analyzed in terms of (1) the performance friction coefficient (μ_p), (2) the fluctuation friction coefficient ($\Delta\mu$), (3) the stability friction coefficient (μ_s), (4) the variability friction coefficient (μ_v), (5) the recovery percentage (%R), and (6) the fade percentage (%F). Among these, μ_p is defined as the average friction coefficient during two fade and recovery cycles. $\Delta\mu$ is defined as the difference between the maximum and minimum value during two fade and recovery cycles. μ_s and μ_v can be calculated according to Formulas (1) and (2) [1,16].

$$\mu_s = \frac{\mu_p}{\mu_{max}} \tag{1}$$
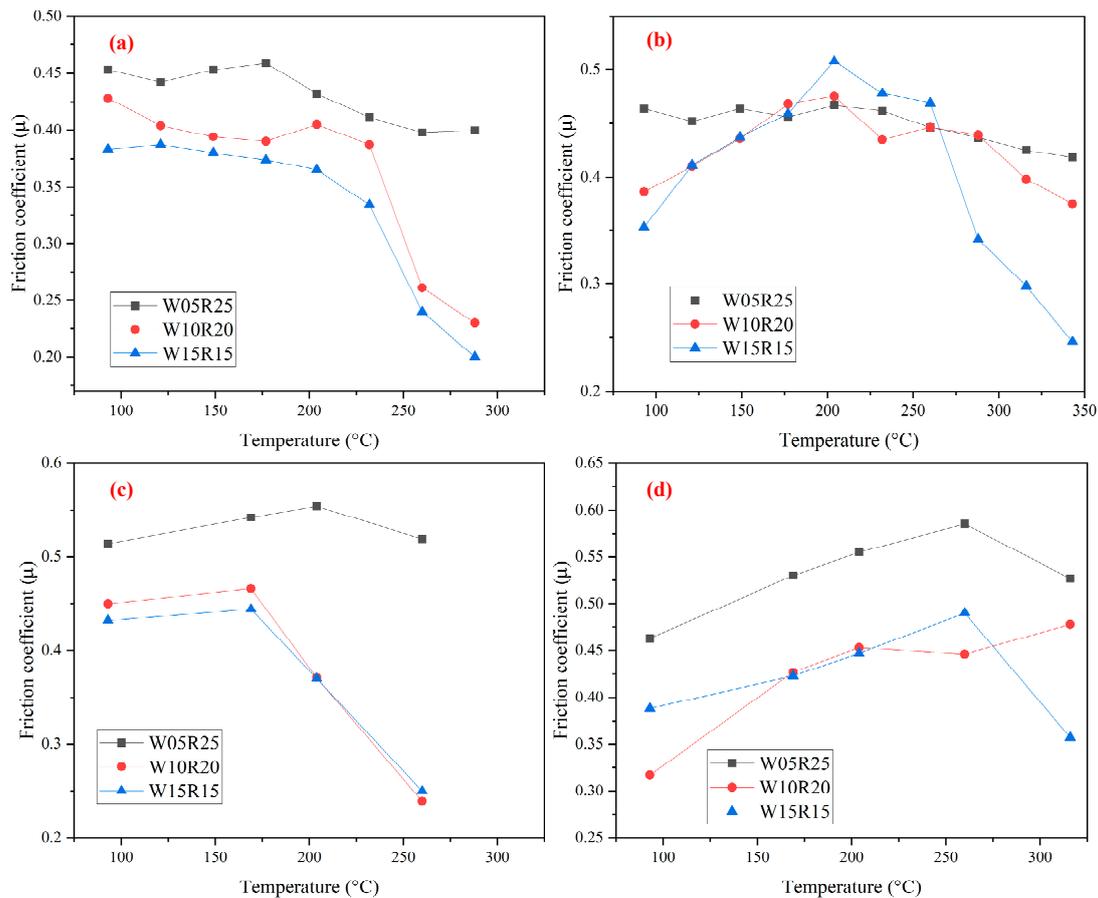
$$\mu_v = \frac{\Delta\mu}{\mu_p} \tag{2}$$

Figure 3. The friction coefficient curves during the fade and recovery cycles of the developed composites: (**a**) Fade-I, (**b**) Fade-II, (**c**) Recovery-I, (**d**) Recovery-II.

3.2.2. μ_p, $\Delta\mu$, μ_s, μ_v Performance of the Composites

Generally, μ_p reflects the overall braking performance of the brake pads, while $\Delta\mu$, μ_s, and μ_v reflect the stability and fluctuation during braking, so, the higher value of μ_p and μ_s and the lower value of $\Delta\mu$ and μ_v can obtain a higher score for the composites [7]. Figure 4 shows the friction coefficient in terms of μ_p, $\Delta\mu$, μ_s, and μ_v for the developed composites. It is found that, with the increase in wood fiber content, the value of μ_p decreases from 0.470 to 0.379; meanwhile, the value of μ_s follows the same trend, with the W05R25 sample having the highest level (0.847), and the W15R15 sample having the lowest level (0.746). The values of $\Delta\mu$ and μ_v have the opposite trend with the increase in wood fiber content for the developed composites. The value of $\Delta\mu$ for the W05R25, W10R20, and W15R15 samples is 0.157, 0.248, and 0.308, respectively. Their μ_v value is 0.344, 0.619, and 0.812. The values of $\Delta\mu$ and μ_v for the W15R15 sample are 50% larger than those of the W05R25 sample.

The higher level of μ_p in the composite with 5% wood fiber content is mainly due to the difference in material composition between wood fiber and rockwool. With the braking processes, the fibers at the friction interface act as a regulator, and the rockwool is sheared into hard abrasives such as silica and alumina, which increase the friction coefficient [27,31]. However, the wood fiber with a large amount of lignin is sheared and changed into coke, which decreases the friction coefficient [32]. The variability of the composites increased with the increase in wood fiber content, mainly due to the low thermal stability of natural fibers, which causes decomposition [17,32].
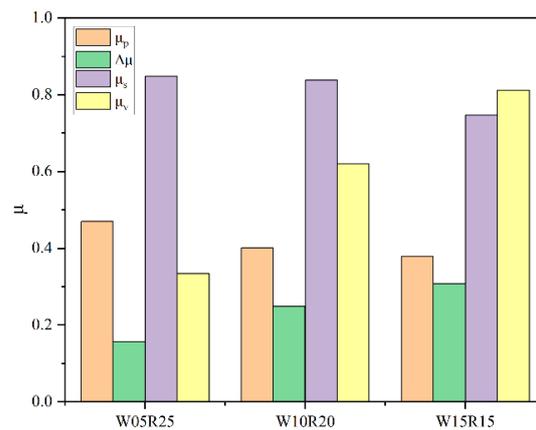
Figure 4. The performance of μ_p, $\Delta\mu$, μ_s, and μ_v.

3.2.3. Fade and Recovery Performance of the Composites

The %F and %R were used to evaluate the fade and recovery properties of composites. The composites with a higher %R and a lower %F are recognized as excellent formula [9,32], and they can be calculated according to Equations (3) and (4) [7,33]:

$$\%F = 1 - \frac{\mu_f}{\mu_p} \tag{3}$$

$$\%R = \frac{\mu_r}{\mu_p} \tag{4}$$

where, μ_f is the lowest value in two fade cycles, and μ_r is the average value in two recovery cycles.

It can be observed from Figure 5 that the value of %F increases with the increase in wood fiber content: the W05R25 sample has the lowest value (15.3), and the %F value for the W10R20 and W15R15 samples is 42.6 and 47.3, respectively, which are nearly three times that of the W05R25 sample. Meanwhile, the %R value follows the opposite trend compared with %F. The W05R25 sample has the highest level (112.3), and the %R value for the W10R20 and W15R15 samples changes very little, namely, 101.2 and 105.4. All three values exceed 100, which demonstrates a better recovery performance [9]. Through the above analysis, it can be obtained that the W05R20 sample has an excellent fade and recovery performance. It is mainly due to the thermal stability of mineral fiber being better than that of natural fiber. With the increase in test temperature, the resin gradually degrades, resulting in a decrease in adhesion, and the mineral fiber is sheared into hard particles to promote friction, which causes lower fade. However, the natural fiber is thermally decomposed into coke, which plays the role of lubrication, causing higher fade [32,34–36].
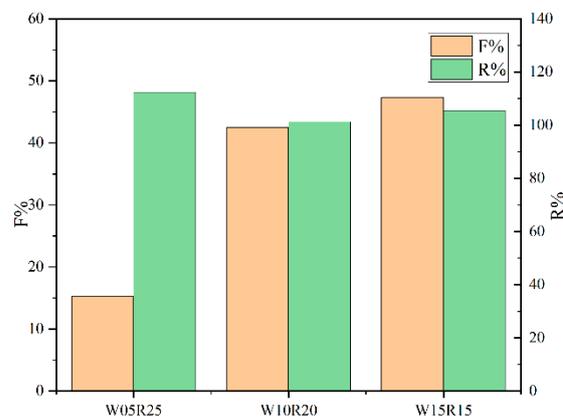

Figure 5. The performance of %R and %F.

3.2.4. Wear Performance of the Composites

Figure 6 shows the wear rate of the three developed composites after the tribology test according to the process in Section 2.3. It can be seen that the mass loss and thickness loss have the same downward trend with the increase in the wood fiber content. The W05R25 sample has the highest wear rate: the mass loss rate and thickness loss rate are 11.32% and 9.8%, respectively. When the wood fiber content achieves 10%, the wear rate has a substantial reduction, and the mass loss rate and thickness loss drop to 4.6% and 4.3%, respectively. However, as the wood fiber content further increases to 15%, the wear rate has a slight decrease, and the mass loss rate and thickness loss rate are 3.81% and 3.67%.
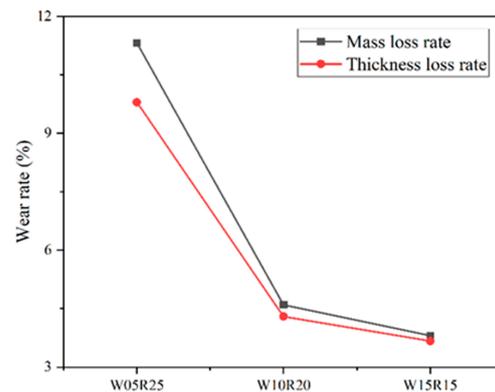

Figure 6. The wear rate of the composites.

It can be explained as follows: rockwool is mainly composed of hard silica and alumina, while wood fiber is mainly composed of soft cellulose and lignin [37,38]. With the increase in temperature and braking, the fibers are sheared as friction property modifiers (abrasives and lubricants). When the content of wood fiber is low, hard particles play a major role in increasing the friction coefficient and wear, but the high content of wood fiber is carbonized into coke, reducing the friction coefficient and wear [32,39]. In general, the addition of a proper amount of wood fiber can reduce the wear rate and improve the wear resistance of friction materials.

3.2.5. Wear Mechanism

It can be known from the previous research on brake friction materials that, with the increase in braking temperature during the test, the resin, rubber, and other organic substances in the composite begin to decompose, causing the surface structure of the composite to loosen. Under the effect of braking pressure, more fibers and hard particles are exposed to the friction surface. However, different components have different effects on the results [1,3]. The worn surface morphology of the three developed braking composites (W05R25, W10R20, and W15R15) characterized by a scanning electron microscope (SU1510, Hitachi Ltd, Tokyo, Japan) is shown in Figure 7.
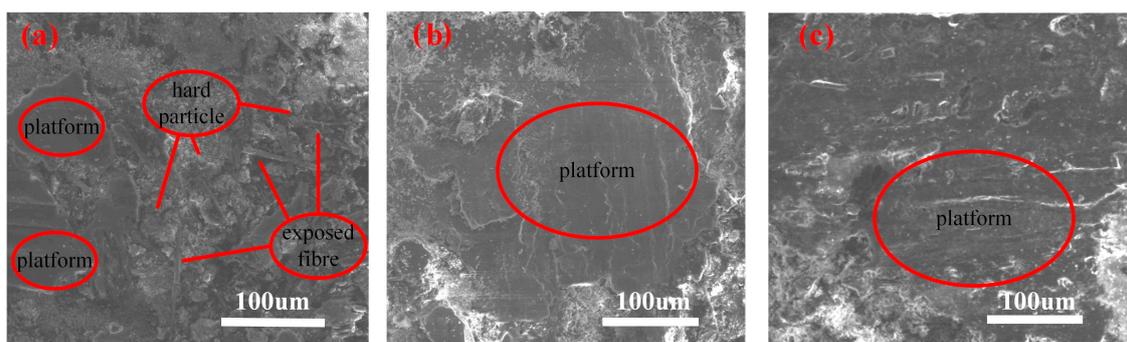

Figure 7. Worn surface morphologies of (**a**) W05R25, (**b**) W10R20, and (**c**) W15R15.

　　　　It can be observed that the worn surface of the W05R25 sample shows a small discontinuous secondary contact platform, a large number of exfoliated fibers, wear debris, and exfoliated pits. It is mainly due to the fact that an increase in temperature and friction causes resin decomposition and fiber exposure, the high content of rockwool causing a large number of hard particles during the friction process, resulting in an increase in the friction coefficient and wear (W05R25 has the highest CoF and wear rate) [21,27]. However, it is quite different from the wear surface of samples W10R20 and W15R15, which are comparatively similar. The worn surface of the W10R20 and W15R15 samples appears to have large continuous contact platforms, less wear debris, and exfoliated fibers. It can be explained that, with the increase in wood fiber content, high-temperature friction causes resin decomposition to loosen the surface, and more wood fibers are exposed to the friction surface, which produces a carbonization effect under instantaneous high-temperature conditions, forming a continuous and complete carbon film, which plays a synergistic lubrication effect with graphite, resulting in the reduction in the friction coefficient and the improvement of the wear resistance in high-temperature conditions [32,35,40].

4. Conclusions

　　　　A total of three asbestos-free brake friction composites with different ratios of wood and rockwool hybrid fibers at a constant total content of 30% were developed. Then, the physical, mechanical, and tribological properties were characterized. Meanwhile, the optimized composition was selected. The results are as follows:

(1)　Density, hardness, and shear strength are higher in samples that contain higher contents of rockwool fiber than wood fiber. Water absorption increases with the increase in wood fiber content.

(2)　Rockwool fiber can improve the coefficient of friction, reduce fluctuation, and enhance friction stability; wood fiber has a significant impact on wear resistance. Meanwhile, the fade performance worsens with the addition of a high content of wood fiber.

(3)　The worn surface of the W05R25 sample showed typical wear characteristics (exposed fibers, small discontinuous platforms, wear debris, and peeling pits); however, in high-content wood fiber samples, large continuous contact platforms appeared.

(4)　The brake friction material with 5% wood fiber and 25% rockwool fiber has the highest stable friction performance (0.847), the highest %R (112.3), the lowest %F (15.3), and the lowest friction variation performance (0.344), which is considered to be the optimal formulation.

Author Contributions: Conceptualization, N.W.; methodology, N.W.; software, F.H.; validation, N.W. and H.L.; formal analysis, H.L.; investigation, N.W.; data curation, N.W.; writing—original draft preparation, N.W.; writing—review and editing, H.L.; funding acquisition, N.W. All authors have read and agreed to the published version of the manuscript.

Data Availability Statement: Not applicable.

References

1.　Wang, N.; Yin, Z. The Influence of Mullite Shape and Amount on the Tribological Properties of Non-Asbestos Brake Friction Composites. *Lubricants* **2022**, *10*, 220. [CrossRef]
2.　Amirjan, M. Microstructure, wear and friction behavior of nanocomposite materials with natural ingredients. *Tribol. Int.* **2019**, *131*, 184–190. [CrossRef]
3.　Ahmadijokani, F.; Shojaei, A.; Dordanihaghighi, S.; Jafarpour, E.; Mohammadi, S.; Arjmand, M. Effects of hybrid carbon-aramid fiber on performance of non-asbestos organic brake friction composites. *Wear* **2020**, *452–453*, 203280. [CrossRef]

4.　Aranganathan, N.; Mahale, V.; Bijwe, J. Effects of aramid fiber concentration on the friction and wear characteristics of non-asbestos organic friction composites using standardized braking tests. *Wear* **2016**, *354-355*, 69–77. [CrossRef]

5.　Kumar, N.; Mehta, V.; Kumar, S.; Grewal, J.S.; Ali, S. Bamboo natural fiber and PAN fiber used as a reinforced brake friction material: Developed asbestos-free brake pads. *Polym. Compos.* **2022**, *43*, 2888–2895. [CrossRef]

6.　Irawan, A.P.; Fitriyana, D.F.; Tezara, C.; Siregar, J.P.; Laksmidewi, D.; Baskara, G.D.; Abdullah, M.Z.; Junid, R.; Hadi, A.E.; Hamdan, M.H.M.; et al. Overview of the Important Factors Influencing the Performance of Eco-Friendly Brake Pads. *Polymers* **2022**, *14*, 1180. [CrossRef]

7.　Kumar, N.; Grewal, J.S.; Kumar, S.; Ali, S.; Kumar, N. A novel Himachal's Bagar (Sabai) grass fiber used as a brake friction material in brake polymer composite and compared to standard brake friction material. *Polym. Compos.* **2022**, *43*, 215–224. [CrossRef]

8.　Kumar, N.; Kumar, S.; Grewal, J.S.; Mehta, V.; Ali, S. Comparative study of Abaca fiber and Kevlar fibers based brake friction composites. *Polym. Compos.* **2021**, *43*, 730–740. [CrossRef]

9.　Monreal, P.; Oroz, J.; Gutiérrez, K.; Ambroj, I.C. Natural Latxa Sheep Wool as an Environmentally Friendly Substitute for Specific Organic Fibers in Railway Friction Materials: A Preliminary Approach. *Tribol. Trans.* **2021**, *64*, 851–863. [CrossRef]

10.　Singh, T.; Tiwari, A.; Patnaik, A.; Chauhan, R.; Ali, S. Influence of wollastonite shape and amount on tribo-performance of non-asbestos organic brake friction composites. *Wear* **2017**, *386–387*, 157–164. [CrossRef]

11.　Cui, G.; Liu, H.; Shi, R.; Li, S.; Han, J. Dry-braking properties of resin based friction materials by different fibres. *Lubr. Sci.* **2019**, *32*, 21–29. [CrossRef]

12.　Hua, Y.; Li, F.; Hu, N.; Fu, S.-Y. Frictional characteristics of graphene oxide-modified continuous glass fiber reinforced epoxy composite. *Compos. Sci. Technol.* **2022**, *223*. [CrossRef]

13.　Struchkova, T.S.; Vasilev, A.P.; Okhlopkova, A.A.; Danilova, S.N.; Alekseev, A.G. Mechanical and Tribological Properties of Polytetrafluoroethylene Composites Modified by Carbon Fibers and Zeolite. *Lubricants* **2021**, *10*, 4. [CrossRef]

14.　Monreal-Pérez, P.; González, J.; Iraizoz, A.; Bilbao, U.; Clavería, I. Effect of the steel fiber length on the friction performance and wear mechanism of railway brake shoes. *Tribol. Int.* **2022**, *172*. [CrossRef]

15.　Jang, H.; Ko, K.; Kim, S.; Basch, R.; Fash, J. The effect of metal fibers on the friction performance of automotive brake friction materials. *Wear* **2004**, *256*, 406–414. [CrossRef]

16.　Ibrahim, M.A.; Hirayama, T.; Khalafallah, D. An investigation into the tribological properties of wood flour reinforced polypropylene composites. *Mater. Res. Express* **2019**, *7*, 015313. [CrossRef]

17.　Mazzanti, V.; Fortini, A.; Malagutti, L.; Ronconi, G.; Mollica, F. Tribological Behavior of a Rubber-Toughened Wood Polymer Composite. *Polymers* **2021**, *13*, 2055. [CrossRef]

18.　Du, G.; Liu, A. The flexural and tribological properties of UHMWPE composite filled with plasma surface-treated wood fibers. *Surf. Interface Anal.* **2017**, *49*, 1142–1146. [CrossRef]

19.　Amirthan, G.; Balasubramanian, M. Reciprocating sliding wear studies on Si/SiC ceramic composites. *Wear* **2011**, *271*, 1039–1049. [CrossRef]

20.　Liu, Y.; Ma, Y.; Lv, X.; Yu, J.; Zhuang, J.; Tong, J. Mineral fibre reinforced friction composites, Effect of Rockwoo fibre on mechanical and tribological behavior. *Mater. Res. Express* **2018**, *5*, 095308. [CrossRef]

21.　Stephen Bernard, S.; Jayakumari, L.S. Effect of rockwool and steel fiber on the friction performance of brake lining materials. *Matéria* **2016**, *21*, 656–665. [CrossRef]

22.　Makni, F.; Cristol, A.-L.; Desplanques, Y.; Elleuch, R. Friction Performance Improvement of Phenolic/Rockwool Fibre Composites: Influence of Fibre Morphology and Distribution. *Materials* **2022**, *15*, 5381. [CrossRef] [PubMed]

23.　Aranganathan, N.; Bijwe, J. Development of copper-free eco-friendly brake-friction material using novel ingredients. *Wear* **2016**, *352–353*, 79–91. [CrossRef]

24.　Bagheri Kazem Abadi, S.; Khavandi, A.; Kharazi, Y. Effects of mixing the steel and carbon fibers on the friction and wear properties of a PMC friction material. *Appl. Compos. Mater.* **2010**, *17*, 151–158. [CrossRef]

25.　Kumar, S.; Mer, K.K.S.; Gangil, B.; Patel, V.K. Synergy of rice-husk filler on physico-mechanical and tribological properties of hybrid Bauhinia-vahlii/sisal fiber reinforced epoxy composites. *J. Mater. Res. Technol.* **2019**, *8*, 2070–2082. [CrossRef]

26.　Song, W.; Park, J.; Choi, J.; Lee, J.J.; Jang, H. Effects of reinforcing fibers on airborne particle emissions from brake pads. *Wear* **2021**, *484–485*, 203996. [CrossRef]

27.　Öztürk, B.; Arslan, F.; Öztürk, S. Hot wear properties of ceramic and basalt fiber reinforced hybrid friction materials. *Tribol. Int.* **2007**, *40*, 37–48. [CrossRef]

28.　Bismarck, A.; Aranberri-Askargorta, I.; Springer, J.; Lampke, T.; Wielage, B.; Stamboulis, A.; Shenderovich, I.; Limbach, H.-H. Surface characterization of flax, hemp and cellulose fibers; Surface properties and the water uptake behavior. *Polym. Compos.* **2002**, *23*, 872–894. [CrossRef]

29.　Ma, Y.; Liu, Y.; Wang, L.; Tong, J.; Zhuang, J.; Jia, H. Performance assessment of hybrid fibers reinforced friction composites under dry sliding conditions. *Tribol. Int.* **2018**, *119*, 262–269. [CrossRef]

30.　Arbelaiz, A.; Fernández, B.; Ramos, J.; Retegi, A.; Llano-Ponte, R.; Mondragon, I. Mechanical properties of short flax fibre bundle/polypropylene composites: Influence of matrix/fibre modification, fibre content, water uptake and recycling. *Compos. Sci. Technol.* **2005**, *65*, 1582–1592. [CrossRef]

31.　Xin, X.; Xu, C.G.; Qing, L.F. Friction properties of sisal fibre reinforced resin brake composites. *Wear* **2007**, *262*, 736–741. [CrossRef]

32. Qi, S.; Fu, Z.; Yun, R.; Jiang, S.; Zheng, X.; Lu, Y.; Matejka, V.; Kukutschova, J.; Peknikova, V.; Prikasky, M. Effects of walnut shells on friction and wear performance of eco-friendly brake friction composites. *Proc. Inst. Mech. Eng. Part J J. Eng. Tribol.* **2014**, *228*, 511–520. [CrossRef]

33. Ali, S.; Kumar, N.; Grewal, J.S.G.; Thakur, V.; Chau, K.W.; Kumar, M. Coconut waste fiber used as brake pad reinforcement polymer composite and compared to standard Kevlar-based brake pads to produce an asbestos free brake friction material. *Polym. Compos.* **2022**, *43*, 1518–1525. [CrossRef]

34. Fu, Z.; Suo, B.; Yun, R.; Lu, Y.; Wang, H.; Qi, S.; Jiang, S.; Lu, Y.; Matejka, V. Development of eco-friendly brake friction composites containing flax fibers. *J. Reinf. Plast. Compos.* **2012**, *31*, 681–689. [CrossRef]

35. Fu, Z.; Yun, R.; Qi, S.; Jiang, S.; Lu, Y. Friction performance and extension evaluation of jute fiberreinforced eco-friendly friction materials. *J. Beijing Univ. Chem. Technol.* **2012**, *39*, 55–59.

36. Matějka, V.; Fu, Z.; Kukutschová, J.; Qi, S.; Jiang, S.; Zhang, X.; Yun, R.; Vaculík, M.; Heliová, M.; Lu, Y. Jute fibers and powderized hazelnut shells as natural fillers in non-asbestos organic non-metallic friction composites. *Mater. Des.* **2013**, *51*, 847–853. [CrossRef]

37. Yap, Z.S.; Khalid, N.H.A.; Haron, Z.; Mohamed, A.; Tahir, M.M.; Hasyim, S.; Saggaff, A. Waste Mineral Wool and Its Opportunities—A Review. *Materials* **2021**, *14*, 5777. [CrossRef] [PubMed]

38. Yang, X.; Berglund, L.A. Structural and ecofriendly holocellulose materials from wood, Microscale fibers and nanoscale fibrils. *Adv. Mater.* **2021**, *33*, 2001118. [CrossRef] [PubMed]

39. Chin, C.W.; Yousif, B.F. Potential of kenaf fibres as reinforcement for tribological applications. *Wear* **2009**, *267*, 1550–1557. [CrossRef]

40. Gehlen, G.S.; Neis, P.D.; Barros, L.Y.; Poletto, J.C.; Ferreira, N.F.; Amico, S.C. Tribological performance of eco-friendly friction materials with rice husk. *Wear* **2022**, *500*, 204374. [CrossRef]